Nanoscale Advances

ROYAL SOCIETY OF CHEMISTRY

PAPER

View Article Online
View Journal | View Issue

Cite this: *Nanoscale Adv.*, 2021, **3**, 5348

Enhanced resistance to decay of imprinted nanopatterns in thin films by bare nanoparticles compared to polymer-grafted nanoparticles†

Sonal Bhadauriya, [a] Asritha Nallapaneni,[a] Xiaoteng Wang, [a] Jianan Zhang, [b] Ali Masud, [c] Michael R. Bockstaller, [b] Abdullah M. Al-Enizi, [d] Christopher M. Stafford, [e] Jack F. Douglas *[e] and Alamgir Karim *[c]

We extend a previous study on the influence of nanoparticles on the decay of nanoimprinted polymer film patterns to compare the effects of "bare" silica (SiO_2) nanoparticles and SiO_2 nanoparticles with grafted polymer layers having the same chemical composition as the polymer matrix. This method involves nanoimprinting substrate-supported polymer films using a pattern replicated from a digital versatile disc (DVD), and then annealing the patterned polymer nanocomposite films at elevated temperatures to follow the decay of the topographic surface pattern with time by atomic force microscopy imaging after quenching. We quantified the relaxation of the pattern height ("slumping") and determined the relaxation time τ for this pattern decay process as a function of nanoparticle filler type and concentration to determine how nanoparticle additives influence relative film stability. Attractive interactions between the bare nanoparticles and the polymer matrix significantly enhance the thermal resilience of the nanopatterns to decay, compared to those of the particle brushes, wherein the particle core interactions are screened from the matrix *via* the brush layer. A novel aspect of this method is that it readily lends itself to *in situ* film relaxation measurements in a manufacturing context. We observe that the relaxation time of the pattern relaxation exhibits entropy–enthalpy compensation in the free energy parameters governing the pattern relaxation process as a function of temperature, irrespective of the NP system used, consistent with our previous experimental and computational studies.

Received 19th March 2021
Accepted 16th July 2021

DOI: 10.1039/d1na00206f

rsc.li/nanoscale-advances

Numerous previous studies have shown that the addition of nanoparticles (NPs) (grafted with polymers to aid in dispersion or bare NPs without grafted polymers) to a polymer matrix alters the glass transition temperature T_g and the viscoelastic behavior of the resultant composite material.[1–3] The underlying reason for this change has been attributed to the altered segmental chain relaxation in the polymer interfacial layer around the NPs.[4] The interaction strength between the NPs and the polymer matrix chains mainly depends on the surface modification of the NPs (unmodified *vs.* polymer grafted) and this quantity is one of the key parameters responsible for the property changes observed in nanocomposites.[5,6] Nanocomposites for which the surface tethered polymers are chemically identical to the matrix polymer are often termed "athermal" blends where the core–core interaction is assumed to be screened by the polymer chains tethered to the NP surface. Our group recently investigated the decay of imprinted features of nanocomposite thin films upon thermal exposure ("slumping") in an athermal blend system[7] where the addition of grafted NPs led to an increased stability of the imprinted features above a certain "compensation temperature", T_{comp}, observed to be in the vicinity of the glass transition temperature of the pure polymer matrix. The compensation temperature refers to a constant of proportionality relating the activation enthalpy and activation entropy compensation in Arrhenius relaxation processes reasonably described by transition state theory. If grafting polymer chains to the NPs is not an option (for economic and/or chemistry related issues), many applications are relegated to chemistries that have highly attractive NP–polymer interactions[8–10] to aid in the dispersion of the NPs. Therefore, it is imperative to also understand how the addition of bare NPs, having attractive interactions with the matrix, influences the slumping behavior of imprinted films, given the

[a]*Department of Polymer Engineering, University of Akron, Akron, Ohio 44325, USA. E-mail: akarim3@central.uh.edu*

[b]*Department of Materials Science and Engineering, Carnegie Mellon University, Pittsburgh, Pennsylvania 15213, USA*

[c]*Department of Chemical and Biomolecular Engineering, University of Houston, Houston, Texas 77204, USA*

[d]*Department of Chemistry, College of Science, King Saud University, Riyadh 11451, Saudi Arabia*

[e]*Materials Science and Engineering Division, National Institute of Standards and Technology, Gaithersburg, Maryland 20899, USA. E-mail: jack.douglas@nist.gov*

† Electronic supplementary information (ESI) available. See DOI: 10.1039/d1na00206f

significant influence that grafted NPs have been shown to have on the relaxation of imprinted films.

Here we present a detailed investigation of the slumping behavior of imprinted poly(methyl methacrylate) (PMMA) (M_n = 3.1 kg mol^{-1}, where M_n is the number average molecular mass) thin films containing two different NP additives, unmodified bare silica (b-SiO_2) NPs (4 to 5 nm in radius) and PMMA-grafted SiO_2 (g-SiO_2) NPs (M_n of the grafted chains ≈19.4 kg mol^{-1} and 7.7 (±2) nm radius). The bulk T_g value of the PMMA matrix ($T_{g,bulk}$) was approximately equal to 97.2 (±0.2) °C, as estimated by ellipsometry.[7] The glass transition of the composite films containing 20% (mass fraction relative to the matrix mass) bare SiO_2 NP PMMA and grafted SiO_2 NPs in the PMMA matrix was 100.3 (±0.5) °C and 99.7 (±0.1) °C, respectively, determined *via* ellipsometry.[11] A pre-patterned polydimethylsiloxane (PDMS) elastomeric stamp was used to imprint parallel lines and space patterns on our neat PMMA thin films and composite thin films containing varying mass fractions of b-SiO_2 NPs and g-SiO_2 NPs (5%, 10% and 20% by mass relative to the matrix mass). Samples after imprinting (PDMS peeled off) had an initial pattern height, H_o of 135 (±5.5) nm and a width of 353 (±0.5) nm. The imprinted films had a residual layer thickness of 36.5 (±6.5) nm underneath the pattern. Patterned samples were characterized *ex situ* by atomic force microscopy (AFM) in terms of the pattern height (H) after the samples were subjected to different annealing temperatures for various exposure times (t). The evolution of the pattern height, H, as a function of exposure time was normalized to the initial pattern height to yield the corresponding decay curves.

The normalized height decay curves comparing 5% and 20% mass fraction (relative to the matrix mass) for the two NP systems, b-SiO_2 and g-SiO_2, can be seen in Fig. 1. It is evident

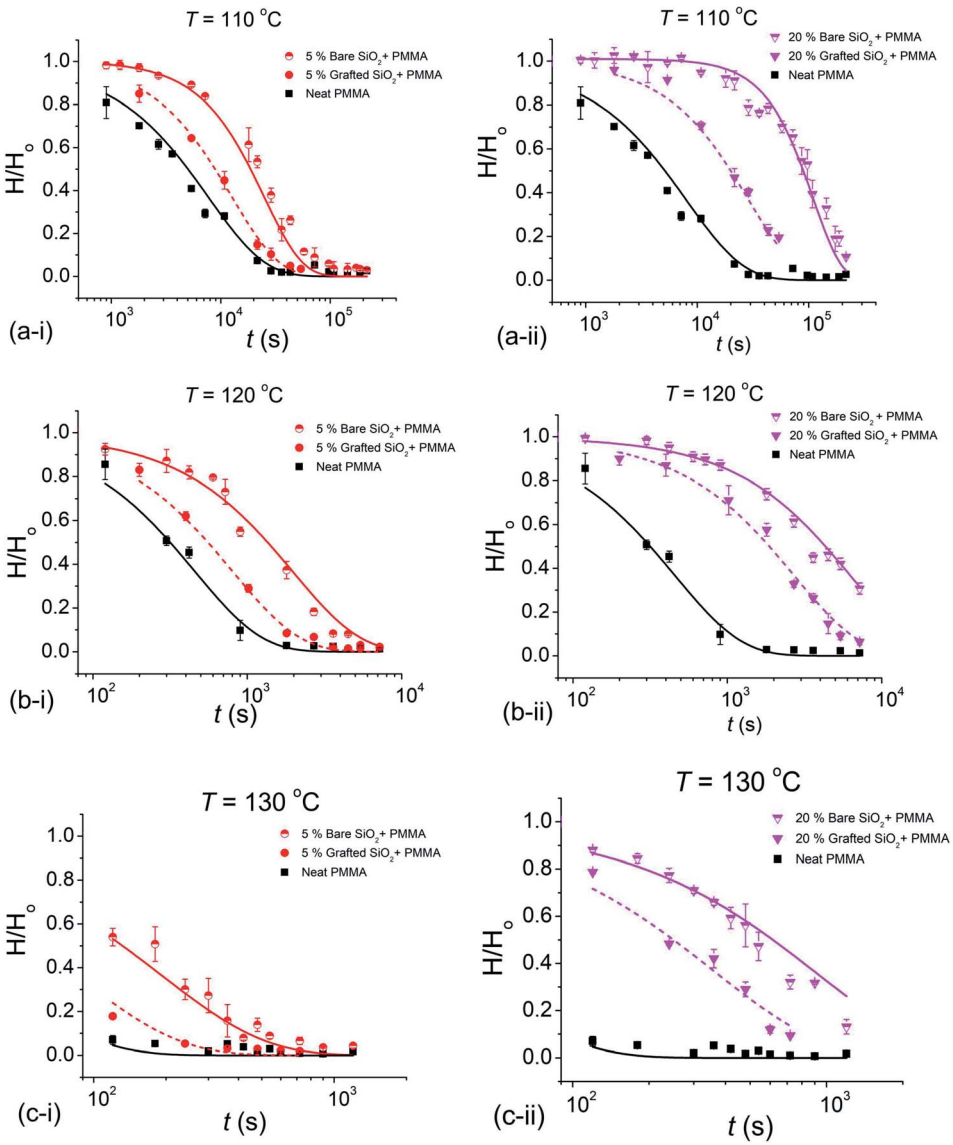

Fig. 1 Decay curves for the normalized pattern height, $H(t)/H_o$ at 110 °C (a-i, a-ii), 120 °C (b-i, b-ii) and 130 °C (c-i, c-ii) for 5% and 20% filled (mass fraction relative to the matrix) b-SiO_2 NP and g-SiO_2 NP filled polymer films. Solid and dashed lines passing through the data points show the generalized exponential fit, and the error bars denote the experimental uncertainty of the measurement.

that the bare b-SiO_2 NPs exhibited substantially better pattern retention than g-SiO_2 NPs. The increase in pattern retention for the b-SiO_2 system can be attributed to the strong interactions between the matrix chains and the unmodified b-SiO_2 NP surface.[8] On the other hand, for the g-SiO_2 NP system, these interacting forces are screened due to the chains grafted on the NP surface, reducing the pattern retention. We also found that as the concentration of the NP additive was increased, better pattern retention was seen, as observed previously for composite films with polymer grafted nanoparticles.[7]

The relaxation data for the normalized pattern height, H/H_o, were fit to a "generalized exponential" function, $H/H_o \approx \exp[-(t/\tau)^{\beta}]$, where t is the waiting time or "exposure time", τ is the "slumping" relaxation time constant and the exponent β quantifies the degree of non-exponentiality of the relaxation process.

The decay curves shown in Fig. 1 indicate a significant stabilization of the imprinted pattern as the volume fraction ϕ of the NPs is increased, which is markedly pronounced for bare nanoparticles. Fitting the reduced pattern height H/H_o to the generalized exponential relaxation function noted above yielded an estimate of the slumping relaxation time τ and β, which quantifies the shape of the relaxation function. Fig. 2 and 3 show the temperature dependence of β and τ for both b-SiO_2 and g-SiO_2 NP filled polymer films. As can be seen from Fig. 2, for the g-SiO_2 NP filled polymer film, β approaches a simple exponential relation ($\beta \approx 1$) at all temperatures investigated. On the other hand, β increases above 1 at low temperatures, but converges to 1 at elevated temperatures for the b-SiO_2 NP system. In our previous study,[7] we observed $\beta > 1$ for clustered PMMA grafted titania nanoparticles at low temperatures. We emphasize that the b-SiO_2 NPs used in the present study are relatively well dispersed, as shown in Fig. S1k–n (see the ESI†) and we do not find any significant clustering. We tentatively associate the values of $\beta > 1$ with highly attractive interactions between the b-SiO_2 NPs and the PMMA matrix, but we must admit that the physical explanation for this unexpected phenomenon is not entirely clear.

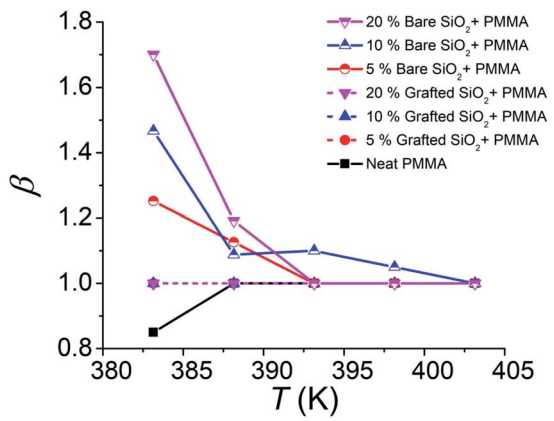

Fig. 2 Variation of the non-exponential relaxation exponent β from the slumping relaxation curves as a function of the NP concentration: 5%, 10% and 20% (mass fractions relative to the matrix) b-SiO_2 and g-SiO_2 NPs in the PMMA matrix. Solid lines show the b-SiO_2 NP system and dashed lines show observations on the g-SiO_2 NP filled polymer film. Dashed lines for 5%, 10% and 20% g-SiO_2 NPs are overlapping.

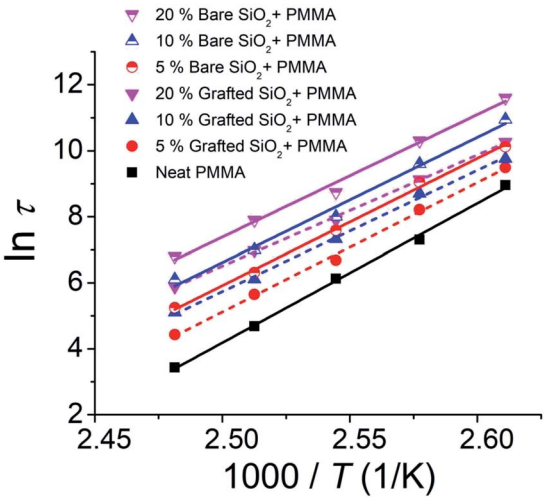

Fig. 3 Temperature dependence of the relaxation time (τ) for 5%, 10% and 20% (mass fractions relative to the matrix) b-SiO_2 and g-SiO_2 NPs in the PMMA matrix. Lines (solid: b-SiO_2 NP filled polymer film; dashed: g-SiO_2 NP filled polymer film) indicate linear fits.

Fig. 3 shows the temperature dependence of the relaxation time τ, whose temperature dependence can be approximated using a linear Arrhenius relation, $\tau = \tau_0 \exp(E_a/RT)$ over the temperature range investigated. We observe three basic trends in our relaxation data: (1) as the concentration of the NP additive is increased, the relaxation time of the pattern decay increases; (2) for a given concentration, the relaxation time for the unmodified NP (b-SiO_2) filled polymer film is higher than that of the grafted NP (g-SiO_2) system; and (3) for both NP types, it seems that the extrapolation of these linear trends leads to a convergence point, similar to our previously observed results for the cluster grafted NP system.[7] Extrapolations of the linear trends for b-SiO_2 and g-SiO_2 NP filled polymer films are shown in Fig. S1h and S2h (see the ESI†), respectively. We observe an approximate intersection point between 2.72 K^{-1} and 2.76 K^{-1} for the g-SiO_2 NP filled polymer film and roughly between 2.96 K^{-1} and 3.03 K^{-1} for the b-SiO_2 NP filled polymer film, corresponding to a T_{comp} of $\approx$ 89.2 °C to 94.5 °C and $\approx$57.4 °C to 64.7 °C, respectively. As apparent in Fig. S1h (see the ESI†), the intersection of the linear trends is not clear for the b-SiO_2 NP filled polymer film compared to that observed for the g-SiO_2 NP filled polymer film in Fig. S2h.† A more robust way of ascribing and interpreting T_{comp} utilizing the convergence plots would be to fully map out the transition region, *i.e.*, the relaxation behavior below and above this characteristic temperature. Probing relaxation behavior for imprinted films below T_g is experimentally challenging due to long relaxation times. We recently probed the relaxation dynamics of wrinkled nanocomposite films and found the T_{comp} to occur in the vicinity of the matrix's T_g.[12] In the present work, the compensation temperature and the deviation range are reported by computing a range of intersection points given by compatible slopes for the linear trends. The T_{comp} values reported from this rough

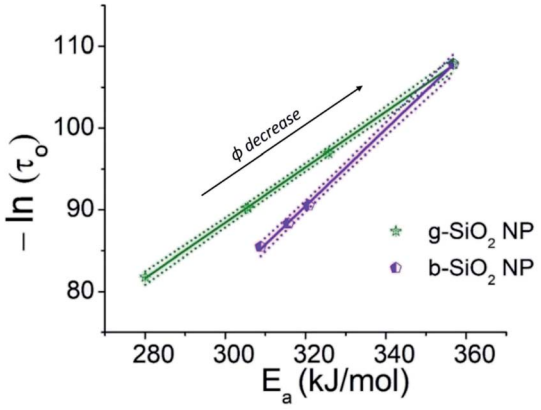

Fig. 4 Entropy–enthalpy compensation (EEC) plot showing the linear dependence between $-\ln(\tau_o)$ and E_a for the b-SiO_2 NP filled polymer film (left-filled violet pentagons, $R^2 \approx 0.999$) and g-SiO_2 NP (crossed-center olive stars, $R^2 \approx 0.999$) filled polymer film. Solid lines represent the linear fits to the data. Dashed lines represent 95% confidence intervals.

estimation of the intersection points for g-SiO_2 and b-SiO_2 NP filled polymer films, respectively, are equal to ≈2 °C to 8 °C and 32.5 °C to 40 °C, which are lower than the bulk glass transition temperature, $T_{g,bulk} \approx 97.24\ (\pm 0.23)$ °C.

The apparent convergence of the relaxation time in Fig. 3 near a compensation temperature occurs when the change in the activation parameters (ΔE_a and ΔS_a) becomes equal, *e.g.*, the relaxation appears to behave as if NPs had not been added (pure polymer). Indeed, we can see the near linearity between $-\ln(\tau_o)$, which is linear in ΔS_a in transition state theory, and E_a for both the unmodified b-SiO_2 NP and grafted g-SiO_2 NP filled polymer films from the data shown in Fig. 4. A similar compensation effect was observed previously for the relaxation of imprinted films with cluster grafted titania NPs.[7] The linearity between the activation parameters of a relaxation process has taken various forms and nomenclatures: the Meyer–Neldel rule, the Constable–Cremer law, an isokinetic relationship, and the entropy–enthalpy compensation effect, as examples. We use the term entropy–enthalpy compensation (EEC) in this work. EEC is an empirical relationship arising in many condensed matter relaxation processes: viscosity of liquids,[13] temperature dependence of fluidity,[14] aqueous solubility of proteins and small molecules,[15] shear viscosity of polymers[16,17] solvent dynamics,[18] antiplasticization by water,[19] relaxation in polymer blends,[20] desiccation tolerance in seeds,[21] temperature dependent specific conductivity,[22–24] relaxation of confined PDMS,[25] oxygen diffusion in the Earth's mantle,[26] heterogeneous catalysis,[27–30] fouling in crude oil,[31] high-frequency dynamics of mixtures,[32] *etc.* Despite decades of study, and its ubiquitous observation in diverse materials, the fundamental origin of EEC remains a topic of theoretical speculation. The most widely accepted interpretation of EEC is that it reflects the rapidly increasing number of paths crossing the transition state barrier in condensed matter relaxation as the barrier heights become large.[33,34] Dyre[33] has reviewed the various arguments for EEC and we have also discussed this phenomenon in our previous work.[7] The existence of EEC requires a clear change in the activation energy (slope of the Arrhenius curve) and an unambiguous tendency for the family of curves to intersect at a common temperature even before any analysis of EEC is made, since otherwise the correlation of the activation energy and prefactor variations could be spurious. This type of analysis is also complicated by complex fluid effects that can make the temperature of relaxation processes and diffusion non-Arrhenius.

The investigation of the compensation phenomenon for pattern relaxation in imprinted films,[7] and the problem of films having variable film thickness[35] where polymer confinement is also involved, leads to the broader fundamental question: why do the activation parameters for a thermally induced pattern decay process linearly compensate each other? The driving force for pattern decay is the surface-energy driven viscous flow[36–38] to reduce the overall surface area of the imprinted films. The activation energy E_a for the relaxation process decreases with

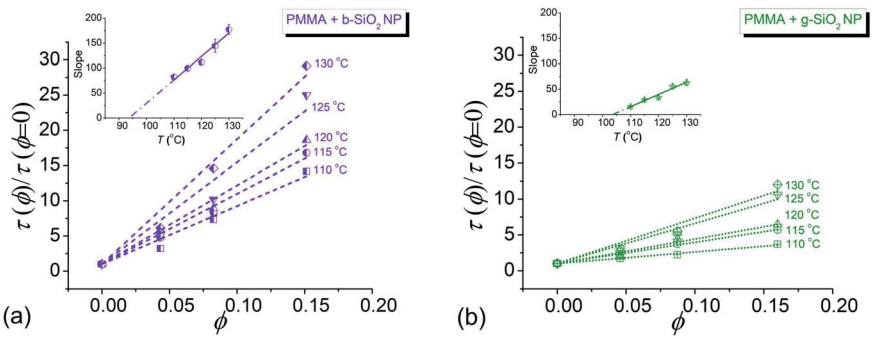

Fig. 5 Relative relaxation time constant of slumping, $\tau_r[\tau(\phi)/\tau(\phi=0)]$, as a function of the (a) b-SiO_2 NPs and (b) g-SiO_2 volume fraction, ϕ. The b-SiO_2 NP system is shown as violet data points: 110 °C, left-filled square; 115 °C, left-filled circle; 120 °C, left-filled upward arrow; 125 °C, left-filled downward arrow; 130 °C, left-filled diamond. The g-SiO_2 NP system is shown as green data points: 110 °C, centered-cross square; 115 °C, centered-cross circle; 120 °C, centered-cross upward arrow; 125 °C, centered-cross downward arrow; 130 °C, centered-cross diamond. Dashed and dotted lines denote linear fits to the data. The inset graph (left-filled violet pentagons for b-SiO_2 NPs and centered-cross greed stars for g-SiO_2 NPs) shows the temperature dependence of the slope and error bars denote the standard error of fitting. $T_{comp} \approx 104$ °C for g-SiO_2 NP and ≈95 °C for b-SiO_2 NP nanocomposite films, respectively.

increasing concentrations of NPs (both unmodified and grafted), whereas the prefactor, $\ln(\tau_o)$, increases (or $-\ln(\tau_o)$, decreases), which can be seen in Fig. S1i and j for the b-SiO_2 NP system and S2i and j for the g-SiO_2 NP system (see the ESI†). To address the occurrence of compensation in slumping relaxation dynamics, a combined theoretical and experimental approach is required. We may obtain an alternate perspective of the entropy–enthalpy compensation effect by plotting our relaxation time relative to the pure material, $\tau_r[\tau(\phi)/\tau(\phi = 0)]$, as a function of the filler volume fraction ϕ and a range of fixed temperatures shown in Fig. 5. It can be inferred from Fig. 5a that the b-SiO_2 NP filled system shows a larger increase in the relaxation time of the patterned structure compared to the g-SiO_2 NP system (Fig. 5b). The insets in Fig. 5a and b show the temperature dependence of the slope where it progressively decreases upon cooling and even approaches 0 as the temperature approaches T_{comp}, which we estimate from the data in Fig. 5 to be near $T_{comp} \approx 104$ °C for the g-SiO_2 NP system and 95 °C for the b-SiO_2 NP system, where both these temperatures are close to T_g of the pure material. Specifically, we found T_g of our bulk PMMA material to be ≈ 97 °C, as reported previously.[7] The strong attractive interaction between the b-SiO_2 NPs and the matrix increases the activation energy of the composite as a whole,[39] but the compensation temperature is observed to be near the glass transition temperature of the pure melt. In some studies investigating glass forming materials, the compensation temperature for relaxation was found to be closer to the Vogel–Fulcher–Tammann (VFT) temperature,[40] T_o, where this temperature is determined from fitting the viscosity (or relaxation time) data to the VFT relation, $\log \eta = A + B/(T - T_o)$. T_{comp} is then estimated from our relaxation time data to be somewhat below (≈ 5 °C) the bulk T_g of the material.[35] This is typical for previous observations of entropy–enthalpy compensation in glass-forming materials.[40]

Conclusions

Understanding the decay of imprinted surface features on a polymer or a polymer nanocomposite thin film presents an important problem in the field of organic nanodevices and smart coatings. The decay behavior of imprinted features is highly influenced by varying the additive system (bare unmodified SiO_2 nanoparticles compared to polymer-grafted SiO_2 nanoparticles); additionally, an entropy–enthalpy compensation behavior is observed in the relaxation dynamics of both nanocomposite materials. Relaxation behavior of patterned polymer surfaces with additives interacting strongly with the matrix leads to a greater persistence of the pattern with time, *i.e.*, greater pattern "stability" above a characteristic compensation temperature (estimated to be ≈ 104 °C for the grafted SiO_2 nanoparticle system and ≈ 95 °C for the bare SiO_2 nanoparticle system). The compensation temperature T_{comp} was observed to be close to T_g of the neat polymer (≈ 97 °C), similar to our previous observations in nanocomposite films containing grafted nanoparticles.[7] The entropy–enthalpy compensation effect is then observed in the pattern relaxation process, irrespective of the additive type, suggesting the robustness of the entropy–enthalpy compensation effect in the dynamics of filled films and films having varying film thickness.[35] The relative ease of tracking the evolution of relief features imprinted on polymer films, both with and without filler particles and other additives, and for general film thickness should make this method useful in materials processing and in service life context where relatively non-invasive measurements can be performed on films *in situ*[11] under conditions where residual stresses, moisture exposure and other complications may also exist.

Experimental section

Poly(methyl methacrylate) (PMMA), M_n 3.1 kg mol^{-1}, polydispersity 1.09 was purchased from Polymer Source (P9059-MMA, syndiotactic rich content >79%) and was used as received. *In situ* ellipsometry measurements to estimate the limiting bulk glass transition were reported previously for this PMMA,[7] leading to a $T_{g,bulk} = 97.2$ (± 0.2) °C. Unmodified bare SiO_2 nanoparticles (b-SiO_2 NPs) (4 nm to 5 nm nominal radius) were purchased from Nissan Chemicals and used as received. The solution is 30% (by mass) colloidal silica mono-dispersed in methyl isobutyl ketone (MIBK), specially catered towards acrylic resins (PMMA in our case) where the surface of this NP has hydroxyl groups, making it highly compatible with our matrix. The glass transition of the composite film containing 20% (mass fraction relative to the matrix mass) bare SiO_2 NPs in the PMMA matrix was 100.3 (± 0.5) °C, determined *via* ellipsometry.[11] The synthesis of PMMA-grafted SiO_2 NPs (g-SiO_2 NPs) was performed utilizing surface-initiated atom transfer radical polymerization.[41,42] The nanoparticles had an average radius of 7.7 (± 2) nm after grafting, as measured by transmission electron microscopy (see ESI, Fig. S3†). The number average molecular mass (M_n) of the grafted PMMA chains was measured to be 19.4 kg mol^{-1} using gel permeation chromatography with a polydispersity of 1.17. The glass transition of the composite film containing 20% (mass fraction relative to the matrix mass) PMMA grafted SiO_2 NPs in the PMMA matrix was 99.7 (± 0.1) °C, determined *via* ellipsometry.[11] The number-average molecular weight (M_n) and molecular weight distribution were determined by size exclusion chromatography (SEC). The SEC was conducted with a Waters 515 pump and Waters 410 differential refractometer using PSS columns (Styrogel 105, 103, and 102 Å) in THF as an eluent at 35 °C and at a flow rate of 1 mL min^{-1}. Linear PMMA standards were used for calibration. Prior to SEC analysis, samples were etched with HF (to remove the silica core) in a polypropylene vial for 20 h, then neutralized with ammonium hydroxide, and subsequently dried with magnesium sulfate before SEC injection. It is noted that the neutralization process has to be conducted with caution under liquid nitrogen to dissipate heat. The PMMA grafting density was estimated to be ≈ 0.65 chains per nm^2 based on the organic mass loss from TGA (see ESI, Fig. S4†).[43]

Neat PMMA solution and composite solutions for the b-SiO_2 NP system and g-SiO_2 NP system (5%, 10% and 20% mass fraction relative to the matrix mass) were prepared in acetone. The solutions were then flow coated onto silicon substrates; the silicon substrates were first cleaned by ultraviolet ozone

treatment for 2 h. The thickness of the films was 104 (±6.5) nm as measured by spectral reflectometry (F-20 Ultraviolet Thin Film Analyzer; Filmetrics, Inc.). Patterned, crosslinked poly(-dimethylsiloxane) (PDMS) elastomer stamps (thickness ≈ 1 mm, 20 : 1 curing ratio) were made by casting the prepolymer against the patterned inset of commercial polycarbonate digital versatile discs (Sony, DVD-R, pitch $\lambda \approx 750$ nm, height difference $\Delta h \approx 135$ nm), subsequently curing at 120 °C for 8 h, and peeling off the patterned PDMS after cooling to room temperature. The patterned elastomeric stamps were then placed in contact with the polymer/polymer composite film and heated at 180 °C for 1 h to transfer the DVD patterns onto the thin film utilizing capillary forces (see ESI, Fig. S5†).[44]

Slumping experiments were conducted at 110 °C, 115 °C, 120 °C, 125 °C and 130 °C. Imprinted samples were placed in a preheated vacuum oven for a prescribed amount of time and rapidly quenched to room temperature upon removal from the oven. The surface topography of the samples before and after slumping was measured using atomic force microscopy (Dimension Icon, Bruker) operated in tapping mode. Multiple AFM scans were taken at random locations on each sample to determine the average height and standard deviation of the slumped pattern height. Representative AFM scans at a slumping temperature of 110 °C are shown in Fig. S6.†

Disclaimer

Certain commercial materials and equipment are identified to specify adequately the experimental procedure. In no case does such identification imply recommendation by the National Institute of Standards and Technology nor does it imply that the material or equipment identified is necessarily the best available for this purpose.

Author contributions

S. B., A. K. and J. F. D. conceived and planned the experiments. S. B., A. N. and X. W. carried out the slumping experiments. J. Z. and M. R. B. contributed to nanoparticle synthesis and characterization. C. M. S. and J. F. D. contributed to the interpretation of the results. S. B. took the lead in writing the manuscript and A. M. and A. M. A. helped review and edit the manuscript. All authors provided critical feedback and helped shape the research, analysis and manuscript.

Conflicts of interest

The authors declare no competing financial interest.

Acknowledgements

A. K. and M. R. B. would like to acknowledge DOE (BES) award DE-SC0018854 for funding of this project. A. K. and A. A.-E. also extend their sincere appreciation to Researchers Supporting Project number (RSP-2021/55), King Saud University, Riyadh, Saudi Arabia for other funding related to the research.

References

1 D. F. Sunday and D. L. Green, *Macromolecules*, 2015, **48**, 8651–8659.
2 D. Kim, S. Srivastava, S. Narayanan and L. A. Archer, *Soft Matter*, 2012, **8**, 10813.
3 J. W. Gu, Q. Y. Zhang, H. C. Li, Y. S. Tang, J. Kong and J. Dang, *Polym.-Plast. Technol. Eng.*, 2007, **46**, 1129–1134.
4 S. Cheng, S.-J. Xie, J. M. Y. Carrillo, B. Carroll, H. Martin, P.-F. Cao, M. D. Dadmun, B. G. Sumpter, V. N. Novikov, K. S. Schweizer and A. P. Sokolov, *ACS Nano*, 2017, **11**, 752–759.
5 Y. Liu, J. Wang, M. Zhang, H. Li and Z. Lin, *ACS Nano*, 2020, **14**, 12491–12521.
6 X. Li, J. Iocozzia, Y. Chen, S. Zhao, X. Cui, W. Wang, H. Yu, S. Lin and Z. Lin, *Angew. Chem., Int. Ed.*, 2018, **57**, 2046–2070.
7 S. Bhadauriya, X. Wang, P. Pitliya, J. Zhang, D. Raghavan, M. R. Bockstaller, C. M. Stafford, J. F. Douglas and A. Karim, *Nano Lett.*, 2018, **18**, 7441–7447.
8 S. Cheng, B. Carroll, V. Bocharova, J. M. Y. Carrillo, B. G. Sumpter and A. P. Sokolov, *J. Chem. Phys.*, 2017, **146**, 203201.
9 F. W. Starr, J. F. Douglas, D. Meng and S. K. Kumar, *ACS Nano*, 2016, **10**, 10960–10965.
10 N. Jouault, M. K. Crawford, C. Chi, R. J. Smalley, B. Wood, J. Jestin, Y. B. Melnichenko, L. He, W. E. Guise and S. K. Kumar, *ACS Macro Lett.*, 2016, **5**, 523–527.
11 S. Bhadauriya, J. Zhang, J. Lee, M. R. Bockstaller, A. Karim, R. J. Sheridan and C. M. Stafford, *ACS Appl. Mater. Interfaces*, 2020, **12**, 15943–15950.
12 S. Bhadauriya, X. Wang, A. Nallapaneni, A. Masud, Z. Wang, J. Lee, M. R. Bockstaller, A. M. Al-Enizi, C. H. Camp, C. M. Stafford, J. F. Douglas and A. Karim, *Nano Lett.*, 2021, **21**, 1274–1281.
13 R. M. Barrer, *Trans. Faraday Soc.*, 1943, **39**, 48–59.
14 C. E. Waring and P. Becher, *J. Chem. Phys.*, 1947, **15**, 488–496.
15 R. Lumry and S. Rajender, *Biopolymers*, 1970, **9**, 1125–1227.
16 D. W. van Krevelen and P. J. Hoftyzer, *Die Angewandte Makromolekulare Chemie*, 1976, **52**, 101–109.
17 J. F. Douglas and W. S. Xu, *Macromolecules*, 2021, **54**, 3247–3269.
18 T. P. Lodge, *J. Phys. Chem.*, 1993, **97**, 1480–1487.
19 C. C. Seow, P. B. Cheah and Y. P. Chang, *J. Food Sci.*, 1999, **64**, 576–581.
20 T. Fahmy and M. T. Ahmed, *Polym. Int.*, 2000, **49**, 669–677.
21 W. Q. Sun, *Plant Physiol.*, 2000, **124**, 1203–1215.
22 E. J. Meijer, M. Matters, P. T. Herwig, D. M. de Leeuw and T. M. Klapwjik, *Appl. Phys. Lett.*, 2000, **76**, 3433–3435.
23 J. C. Wang and Y. F. Chen, *Appl. Phys. Lett.*, 1998, **73**, 948–950.
24 H. Schmidt, M. Wiebe, B. Dittes and M. Grundmann, *Appl. Phys. Lett.*, 2007, **91**, 232110.
25 A. Schonhals, C. Schick, B. Frick and R. Zorn, *Eur. Phys. J. E*, 2003, **12**, 173–178.
26 S. M. Fortier and B. J. Giletti, *Science*, 1989, **245**, 1481–1484.

27 T. Bligaard, K. Honkala, A. Logadottir, J. K. Nørskov, S. Dahl and C. J. H. Jacobsen, *J. Phys. Chem. B*, 2003, **107**, 9325–9331.
28 C. E. Ramachandran, B. A. Williams, J. A. Van Bokhoven and J. T. Miller, *J. Catal.*, 2005, **233**, 100–108.
29 J. A. Van Bokhoven, B. A. Williams, W. Ji, D. C. Koningsberger, H. H. Kung and J. T. Miller, *J. Catal.*, 2004, **224**, 50–59.
30 D. Teschner, G. Novell-Leruth, R. Farra, A. Knop-Gericke, R. Schlogl, L. Szentmiklosi, M. G. Hevia, H. Soerijanto, R. Schomacker, J. Perez-Ramırez and N. Lopez, *Nat. Chem.*, 2012, **4**, 739–745.
31 C. A. Bennett, R. S. Kistler, K. Nangia, W. Al-Ghawas, N. Al-Hajji and A. Al-Jemaz, *Heat Transfer Eng.*, 2007, **RP5**, 32–42.
32 T. Psurek, C. L. Soles, K. A. Page, M. T. Cicerone and J. F. Douglas, *J. Phys. Chem. B*, 2008, **112**, 15980–15990.
33 J. C. Dyre, *J. Phys. C: Solid State Phys.*, 1986, **19**, 5655–5664.
34 J. R. Macdonald, *J. Appl. Phys.*, 1987, **61**, 700–713.
35 J. Y. Chung, J. F. Douglas and C. M. Stafford, *J. Chem. Phys.*, 2017, **147**, 154902 (1–8).
36 J. Teisseire, A. Revaux, M. Foresti and E. Barthel, *Appl. Phys. Lett.*, 2011, **98**, 013106.
37 K. J. Alvine, Y. Ding, J. F. Douglas, H. W. Ro, B. C. Okerberg, A. Karim and C. L. Soles, *Soft Matter*, 2009, **5**, 2913–2918.
38 K. J. Alvine, Y. Ding, J. F. Douglas, H. W. Ro, B. C. Okerberg, A. Karim, K. A. Lavery, S. Lin-Gibson and C. L. Soles, *J. Polym. Sci., Part B: Polym. Phys.*, 2009, **47**, 2591–2600.
39 F. W. Starr and J. F. Douglas, *Phys. Rev. Lett.*, 2011, **106**, 115702.
40 B. A. P. Betancourt, P. Z. Hanakata, F. W. Starr and J. F. Douglas, *Proc. Natl. Acad. Sci. U. S. A.*, 2015, 1418654112 (1–6).
41 J. Pyun and K. Matyjaszewski, *Chem. Mater.*, 2001, **13**, 3436–3448.
42 K. Matyjaszewski and N. V. Tsarevsky, *Nat. Chem.*, 2009, **1**, 276–288.
43 M. Schmitt, J. Zhang, J. Lee, B. Lee, X. Ning, R. Zhang, A. Karim, R. F. Davis, K. Matyjaszewski and M. R. Bockstaller, *Sci. Adv.*, 2016, **2**, e1601484.
44 Y. Xia and G. M. G. Whitesides, *Annu. Rev. Mater. Sci.*, 1998, **28**, 153–184.